The Journal of Experimental Biology 201, 1659–1671 (1998)
Printed in Great Britain © The Company of Biologists Limited 1998
JEB1525

MYOTOMAL SLOW MUSCLE FUNCTION OF RAINBOW TROUT *ONCORHYNCHUS MYKISS* DURING STEADY SWIMMING

LUCY HAMMOND[1], JOHN D. ALTRINGHAM[1,*] AND CLEMENT S. WARDLE[2]

[1]*School of Biology, University of Leeds, Leeds LS2 9JT, UK* and [2]*SOAEFD Marine Laboratory, PO Box 101, Aberdeen AB9 8DB, UK*

*Author for correspondence (e-mail: j.d.altringham@leeds.ac.uk)

Accepted 26 February; published on WWW 27 April 1998

Summary

Strain and activity patterns were determined during slow steady swimming (tailbeat frequency 1.5–2.5 Hz) at three locations on the body in the slow myotomal muscle of rainbow trout *Oncorhynchus mykiss* using sonomicrometry and electromyography. Strain was independent of tailbeat frequency over the range studied and increased significantly from ±3.3 % l_0 at 0.35*BL* to ±6 % at 0.65*BL*, where l_0 is muscle resting length and *BL* is total body length. Muscle activation occurred significantly later in the strain cycle at 0.35*BL* (phase shift 59 °) than at 0.65*BL* (30 °), and the duration of activity was significantly longer (211 ° at 0.35*BL* and 181 ° at 0.65*BL*). These results differ from those of previous studies. The results have been used to simulate *in vivo* activity in isolated muscle preparations using the work loop technique. Preparations from all three locations generated net positive power under *in vivo* conditions, but the negative power component increased from head to tail. Both kinematically, and in the way its muscle functions to generate hydrodynamic thrust, the rainbow trout appears to be intermediate between anguilliform swimmers such as the eel, which generate thrust along their entire body length, and carangiform fish (e.g. saithe *Pollachius virens*), which generate thrust primarily at the tail blade.

Key words: muscle, fish, swimming, rainbow trout, *Oncorhynchus mykiss*, electromyography, sonomicrometry, work loop.

Introduction

As a fish swims, a wave of body curvature is produced through the combined effect of muscle activity and the interaction of the body with water. The body develops a reactive thrust which pushes the fish forward. Kinematic studies of steady swimming have shown differences in the wave of curvature produced during swimming in different species (Gray, 1933*a*; Webb, 1971; Grillner and Kashin, 1976; Hess and Videler, 1984; Rome *et al.* 1993). It is likely that the variety of different body forms that exist in fish may be related to a number of different modes of swimming and hence methods of generating power. Indeed, kinematic analyses have led to the conclusion that power generated by muscle contraction may be transferred to the water in a number of ways, from continuously along the body to discrete pulses from the tail blade (Lighthill, 1971; Hess and Videler, 1984; Carling *et al.* 1994). These generalisations are complicated by the many other specialised functions of muscle in posture control and the manoeuvre repertoires of each species.

During steady swimming, lateral muscle fibres shorten and lengthen rhythmically. The timing of muscle activity during the shortening and lengthening cycle determines the force, work and power output of a muscle (Altringham and Johnston, 1990; Josephson, 1993). Differences in the phase between muscle activation and the strain cycle recorded *in vivo* (Grillner and Kashin, 1976; Williams *et al.* 1989; van Leeuwen *et al.* 1990; Wardle and Videler, 1993; Jayne and Lauder, 1995) suggest that the mode of muscle function may change along a fish body and vary between species. By applying the work loop technique developed by Josephson (1985), *in vitro* studies mimicking *in vivo* conditions have been performed on several species, using isolated fast and slow lateral muscle fibres from different positions along the body (Altringham *et al.* 1993; Rome *et al.* 1993). These studies show that the phase relationship between strain and activation cycles along the fish length plays an important role in the way in which muscle functions.

Rainbow trout swim predominantly by undulation of their body and appear to produce a significant amount of thrust from the tail blade. Pioneering kinematic and electromyogram (EMG) studies of rainbow trout (Williams *et al.* 1989) have derived the timings of muscle activity during the strain cycle *in vivo*. However, the results show interesting differences from those from other species (Wardle *et al.* 1995). Stimulated by these differences, we have measured directly muscle length changes and activity at three body positions in rainbow trout during steady swimming, using sonomicrometry and electromyography. We then carried out work loop studies (performed on isolated slow

muscle preparations from the same three locations) using the *in vivo* parameters determined in this study. These could then be compared with findings for other carangiform swimmers. In addition, a systematic work loop investigation was made of the effects of changing cycle frequency, phase shift and other important parameters. These results have been used to describe how the rainbow trout uses its lateral slow muscle to swim and how its swimming mode compares with those of other species studied in this way.

Materials and methods

Sonomicrometry and electromyography

Rainbow trout *Oncorhynchus mykiss* (Walbaum) were reared from eggs at Aultbea Marine Laboratory (SOAEFD), Scotland, UK. Four weeks before experimentation, 20 individuals (38–45 cm total length *BL*) were moved to a 10 m×1.5 m (diameter × height) seawater tank at 11 °C at the SOAEFD Marine Laboratory, Aberdeen. Trout were fed sand eels daily. Farmed fish often incur some damage to their fins as a result of the high rearing densities. Only individuals with completely intact caudal fins were selected for this experiment. Four or five fish were selected to form a study group by dividing the tank in half using fabric barriers to form the swimming area.

Simultaneous sonomicrometry and EMG recordings were made from three longitudinal positions in slow muscle along the body of a trout. EMG electrodes were constructed from 0.125 mm diameter insulated copper wire. Insulation was removed over a 2 mm portion at the electrode tip. Bipolar electrodes were used at each recording point. Signals were referred to an external plate placed in the swimming tank. Preamplifiers (Universals, Gould) were placed on the edge of the tank. Signals were amplified with high- and low-pass filters set at 30 and 300 Hz, respectively, and a 50 Hz notch was used to reduce mains interference. Periodic checks were made to see whether the filters were removing any of the source signal as well as any other extraneous noise, by removing the high- and low-pass filters. Sonomicrometry determines the distance between a pair of transducers (piezoelectric ceramic crystals) by measuring the 'transit time' of an ultrasonic (3–5 MHz) pulse (Triton Technology, SD, USA).

In each experiment, three pairs of sonomicrometry transducers and three pairs of EMG wires were used. Extensions (up to 9 m long) of bathythermograph wire (Sippican Blue, MA, USA) were added to each wire in order to connect to the sonomicrometry and EMG preamplifiers. This wire is composed of pairs of very fine (0.065 mm in diameter) individually insulated copper wires. By using very fine wire on large experimental animals, we endeavoured to minimise any drag caused by trailing wires from the fish. Risk of cross-talk between channels was minimised by keeping the paired electrodes at each of the three body positions within each figure-of-eight wire pair. Nine figure-of-eight wire pairs were required, and these were bundled together using an adhesive of Perspex and chloroform spotted at approximately 10 cm intervals. Reduction of any signal interference between the fish and preamplifiers was achieved by minimising wire length and making all joints as clean as possible. Joints between wires and electrodes were cleaned thoroughly with phosphoric acid and then soldered together using phosphoric acid as a flux. All joints were insulated with a Perspex/chloroform mixture.

To allow insertion of the sonomicrometry transducers in the correct plane and precise depth within the fish, 7 mm cross bars of monofilament nylon line (1 mm diameter) were attached to the wire insulation using epoxy adhesive. Cross bars were aligned parallel to the face of the transducer and perpendicular to the leads from it. The twisted, flexible leads between the cross bar and transducer allowed the transducers to move with the muscle, and they were not affected by skin displacement where the cross bars were sutured.

Surgical preparation

An individual fish was removed from the study group and placed in a tank containing MS222 at a concentration of $0.1\,g\,l^{-1}$ sea water until fully anaesthetised (approximately 5 min). The anaesthetised fish was then placed on a 'wet table', and the gills were perfused with aerated anaesthetic ($0.0375\,g\,l^{-1}$) in sea water at 11 °C and at a flow rate of $10\,l\,min^{-1}$. The total period of anaesthesia was limited to 40 min including administration and recovery.

Pairs of 1 mm unlensed sonomicrometry transducers (VD-5, Triton Technology, SD, USA) were introduced into the slow muscle at the lateral line (where fibre orientation is parallel to the surface). Pairs of transducers were introduced 0.35, 0.5 and 0.65*BL* from the rostral tip. Each pair was separated by approximately one myotome (approximately 1 cm) width. At the point of tranducer insertion, a puncture was made using a 1.1 mm diameter hypodermic needle in the direction of the spine, and transducers were introduced directly into the hole. After implantation, the cross bars were sutured into place on the skin surface. Pairs of EMG electrodes were inserted approximately 1 cm apart (*via* a chamfered hypodermic needle) into the slow muscle at each location, within 3 mm of the transducers. Their final position was slightly ventral to the sonomicrometry transducers, with all elements in the same myotome. At its exit from the skin, the electrode wire was sutured into place to avoid any displacement within the muscle. The trailing wires were brought together and sutured ventrally to the skin near to the anus.

After surgery, the gills were perfused with sea water until normal opercular activity resumed. Once the fish had recovered sufficiently, it was returned to the main tank and allowed to swim freely around the tank, rejoining the 3–4 undisturbed individuals for 1 h until the study started.

Rigor measurements

Once sufficient data had been collected, the fish was captured and killed by administration of a lethal dose of MS222, laid flat and allowed to go into rigor. The exact positions of transducers were measured at the skin surface

before the transducers were removed and replaced with plastic markers. Blocks were cut from the fish, and the tissue was fixed in 50 % formalin in Ringer's solution, and transducer separation and positions on the body surface were measured and recorded. After fixing, measurements were made by dissection to determine the depth of the transducer pairs, the distance between them, and their alignment with respect to fibre orientation. Records taken using transducers misaligned by more than 10 ° to the fibre long axis plane were discarded. Positions of EMG electrode tips and sonomicrometry transducers were noted with respect to myotome and fibre type. Results were used only if both EMG electrodes and sonomicrometry transducers were in the slow muscle and clear of the slow/fast muscle junction.

Video recording

A 50 Hz CCD video camera with a 15 mm lens positioned above the tank recorded the fish swimming across the tank throughout EMG and sonomicrometry recordings. The field of view allowed approximately eight body lengths to be seen. A video mixer was used to superimpose the continuous sonomicrometry and EMG signals on the image of the swimming fish, to synchronise all measurements. To allow precise synchronisation of all data, an extra data channel was used to record a random electrical pulse which powered a light-emitting diode (LED) on the video screen. All filming was recorded on S-VHS video tape at 50 Hz.

Data collection and analysis

The aim was to record at three points along the rainbow trout body both the muscle strain cycle and the time of onset and end of the EMG signal during swimming at a steady speed. The d.c. output of the sonomicrometer (Triton 120.2, Triton Technology, SD, USA) and the EMG signals were converted using an analogue-to-digital (A/D) converter (1401, Cambridge Electronic Design) and recorded using Spike 2 software (Cambridge Electronic Design) onto a PC microcomputer. Fish are unpredictable in their swimming behaviour, and a lengthy sampling period was required in order to include bouts of swimming showing a range of different steady speeds. We found that an A/D sampling rate of only 1000 Hz allowed records from seven analogue channels to be recorded as a manageable file, monitoring 512 s of observation. The sampling cycle took 7 ms, with each of the seven channels sampled 143 times per second. The six other channels were the three amplified and filtered EMG channels and the three sonomicrometer channels. Timing synchrony of the seven signals was therefore accurate to 7 ms, or all samples were within approximately 2.5 ° of phase at 1 tailbeat s^{-1} (or 0.7 % tailbeat period). At these relatively slow sampling rates, each of the EMG channels shows a zero activity baseline level when the muscle is inactive and a relative displacement of the EMG signal level when action potentials are present: this displacement time was sufficient to reveal the time of onset and end of the burst of activity but not its detailed structure. The voltage levels of the three sonomicrometer channels for the same positions and times give smooth curves which are calibrated to represent the instantaneous muscle strains.

Regions of film were selected from the video recording that showed steady swimming sequences at constant speeds over four tailbeats in a straight line. The corresponding sonomicrometry and EMG outputs were then analysed using Spike 2 software.

During each sequence of steady swimming, the time and amplitude of maximum and minimum strains were recorded for each tailbeat. These were allocated phases of 90 ° and 270 °, respectively, in the length-change cycle, and the onset and offset of EMG activity were calculated with respect to these phases for each tailbeat. Strain amplitude (as percentage change of resting muscle fibre length l_0) was measured as half the difference between maximum and minimum values. For each sequence of steady swimming, the average values of strain amplitude, the times for EMG onset and EMG offset and EMG duration for each of the four tailbeats were measured.

Calibration of the sonomicrometry signal was made from direct measurement in fresh water/Ringer's solution, with correction for the slightly greater sound transmission speed in muscle (1522–1572 m s^{-1}) relative to water (1500 m s^{-1}) (Goldman and Richards, 1954; Moi and Breddels, 1982). Skeletal muscle changes density when contracting, but the change in the speed of sound transmission has been shown to be small (Griffiths, 1987; Hatta *et al.* 1988).

Kinematic analysis

In order to check that wired fish were swimming normally, analysis of selected video sequences was carried out over the middle two of at least four steady tailbeats of both wired and unwired fish. Frames were transferred to a PC microcomputer every 0.02 s from S-VHS video using frame-grabbing software (MS Video for Windows and Videoblaster RT300 card). The resolution of the video frames was 640 pixels × 480 pixels, giving a resolution of up to ±8 mm. The mean path of motion was referred to as the *x*-axis in a frame of reference; the *y*-axis was perpendicular to this. The positions of the head and tail tips were marked. Displacements of the head in the *x* direction were calculated for every frame (i.e. at 50 Hz). Stride length (distance travelled in the *x* direction per tailbeat/body length) was measured from wired and unwired fish for a number of different tailbeat frequencies.

Muscle mechanics

Mechanical experiments were carried out in Leeds, UK. Fish of 27–32 cm total length (*BL*) were reared at Kilnsey Trout Farm, North Yorkshire, UK, and maintained in filtered, recirculating water at 11 °C for up to 3 weeks before experiments. Individuals were killed by a blow to the head and the brain quickly destroyed. Bundles of fibres were removed from close to the lateral line at 0.35, 0.5 and 0.65*BL* from the rostral tip. Slow fibres were dissected in Ringer's solution (109 mmol l^{-1} NaCl, 2.7 mmol l^{-1} KCl, 2.5 mmol l^{-1}

$NaHCO_3$, 1.8 mmol l^{-1} $CaCl_2$, 0.47 mmol l^{-1} $MgCl_2$, 5.3 mmol l^{-1} sodium pyruvate, 10 mmol l^{-1} Hepes, pH 7.4 at 6 °C). Bundles of fibres approximately 1–2 mm in diameter and 3–4 mm long between the two myosepta were used. These were attached directly *via* connective tissue at each end of the muscle bundle to a servo arm and force transducer (AE801, SensoNor, Horten, Norway) within the chamber of the work loop apparatus and left to rest for 1 h to recover from any trauma caused during dissection. Muscle preparations were bathed in circulating Ringer's solution at 9 °C for the duration of the experiment. The work loop apparatus and techniques were as previously described (e.g. Altringham and Johnston, 1990).

Each muscle preparation was initially set to approximately resting length. Stimulation amplitude (2 ms pulses) was adjusted to 120 % of that giving a maximum twitch response. The resting length (l_0) of the fibres was then adjusted to yield the maximum twitch response. The stimulation frequency yielding a maximum tetanic response was determined (100 Hz) and showed minimal variation; this was used in subsequent work loop experiments. The maximum tetanic stress (P_0) and twitch kinetics [time from stimulus to peak force (t_a) and time from stimulus to 10 % of peak force during relaxation (t_{90})] were measured at this length.

Muscle preparations were subjected to sinusoidal length changes symmetrical about l_0 and stimulated phasically over four cycles. Stimulation onset and duration and the frequency of the strain cycle were derived from our *in vivo* investigations. We were also able to extract approximate timings from a preliminary study by Williams *et al.* (1989) for comparison. A further investigation determined those parameters required for maximum work and power production, using protocols described previously (Altringham and Johnston, 1990; Altringham *et al.* 1993). A period of 6 min was allowed between each experimental run to allow the preparation to recover and to minimise fatigue. At the time of experimentation, no data were available on muscle strain amplitude in rainbow trout at each of the positions studied. Therefore, strains were chosen that were similar to those measured in other carangiform fish; ±3, 4 and 5 % l_0 were used for preparations from 0.35, 0.5 and 0.65*BL* positions, respectively, in all experiments.

Power output (determined using the work loop technique, Josephson, 1985) reached a steady state after the first cycle. Work and power output were derived from the third cycle. At the end of the study, the muscle was removed from the chamber and blotted to remove Ringer's solution. Using a stereomicroscope, all connective tissue was cut away, and the muscle preparation was weighed.

To monitor change in muscle performance over the experimental period, preparations were subjected to a control trial, with a fixed set of parameters, after every three experimental trials. Power outputs for all trials were scaled relative to any change in power output measured in the control trial. It was found that power output sometimes increased by up to 50 % after the first 30 min of a trial. After this initial period, muscle performance was stable and little change was observed over the next 10 h. The 2 °C difference in temperature between the *in vivo* and *in vitro* studies had a negligible effect on isometric kinetics, and studies on tuna *Thunnus albacares* (Altringham and Block, 1997) suggest that temperature-induced changes in optimal stimulation phase shift will be very small for this temperature difference.

Statistical analyses

Statistical analyses were carried out using SigmaStat (Jandel Scientific, San Diego) software or Minitab. For each fish, a Pearson product moment correlation test was performed to investigate the relationship between strain and EMG onset and offset, with tailbeat frequency, at each body position. A two-factor general linear model (GLM) was used to investigate the variation of muscle strain along the body (with fish and body position as the two factors), since the number of determinations of strain varied between both fish and body position, precluding the use of a two-way analysis of variance (ANOVA). Stride length was compared between wired and unwired fish using a Student's *t*-test. Basic mechanical properties (t_a, t_{90}, P_0 and maximum power output) were tested for significant differences between body positions using a one-way ANOVA. Significant differences were measured using the Student–Newman–Keuls test. All results are expressed as mean ± S.E.M., with the mumber of observations given in parentheses.

Instantaneous power output calculations

Instantaneous power output of muscle preparations was calculated as the product of force and shortening velocity. Shortening velocity was derived from dx/dt, where x is the distance the muscle shortened about l_0 and t is time.

Results

Kinematic comparison of wired and unwired fish

A kinematic comparison of wired and unwired fish revealed no significant difference (P>0.05) in stride length (distance travelled per tailbeat/*BL*) at a given tailbeat frequency (approximately 2 Hz). Stride length was 0.64±0.01 in wired fish and 0.63±0.01 in unwired fish (N=7), compared with 0.65 measured by Webb *et al.* (1984) and Webb (1988). Thus, the addition of recording wires to the fish did not appear to lead to a significant increase in drag and corresponding changes in swimming kinematics.

Strain measurements

Sonomicrometry sequences from straight, steady swimming (i.e. at a constant tailbeat frequency for four or more tailbeats) were analysed over a range of tailbeat frequencies between 1.5 and 2.7 Hz. Below these frequencies, undulatory swimming movements were unsteady and pectoral fin swimming was often observed. A fast-Fourier analysis was carried out on selected sequences using MATLAB software and showed that muscle strain during the

length-change cycle approximated a sine wave. Within steady swimming sequences, each tailbeat was therefore described as a sine wave where resting lengths were 0 °/360 ° during lengthening and 180 ° during shortening.

Strain was independent of tailbeat frequency in every fish studied (N=11–30 for 3–4 fish), between 1.5 and 2.7 Hz, at a given location (Fig. 1A). There was no significant difference (P=0.97, GLM) in strain between fish at corresponding body positions (N=3 fish for which data were available from all three body locations), but a highly significant difference was found between different body positions (P<0.001, GLM), with no significant interaction between the two variables (P=0.26). The mean strain of slow fibres increased from ±3.3±0.07 % l_0 at 0.35*BL* to ±6.0±0.05 % l_0 at 0.65*BL* (Fig. 1B).

Relationship between bending and activation waves

Simultaneous sonomicrometry recordings from all three points show that the time course of the bending wave was not linear, but that the wave accelerated as it reached the posterior region of the fish (Figs 2, 3). Propagation of the wave of activation accelerated along the fish length and travelled faster than the bending wave (Fig. 3). This resulted in a small phase difference in muscle activity during the length-change cycle at each body position (Fig. 3).

The onset of activation occurred late in the lengthening phase at each body position and continued as muscle shortened (Figs 2, 3). Once the EMG onset and offset times for that tailbeat were known, then the strain phase shift at these two times was determined. The period (duration) when the muscle was electrically active could thus be related to the strain cycle. As tailbeat frequency increased, there was no significant change (P>0.05) in the onset, offset or duration (as a proportion of the tailbeat) of EMGs at each position for each fish (N=7–16 for each fish) (Fig. 4). Activation occurred significantly earlier in the length-change cycle (P<0.05) at more caudal positions: 59±0.9 ° at 0.35*BL* (N=3 fish), 40±0.4 ° at 0.5*BL* (N=4 fish) and 30±0.2 ° at 0.65*BL* (N=4 fish). The duration of activity within the tailbeat cycle decreased significantly from head to tail (P<0.05): 211±1.2 ° at 0.35*BL*, 190±1.2 ° at 0.5*BL* and

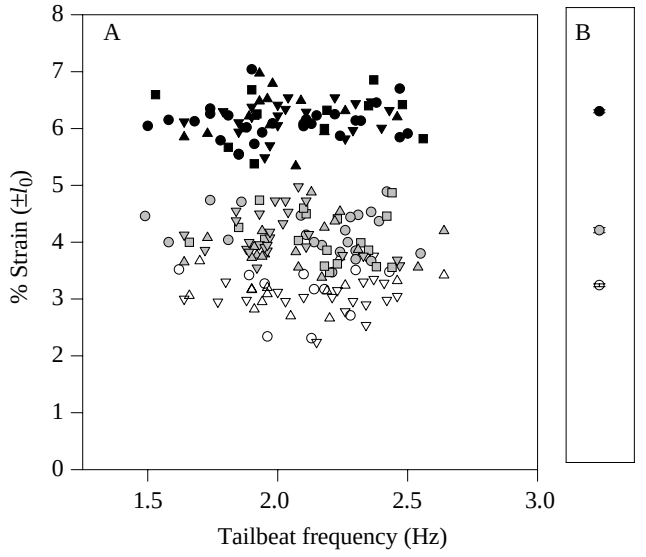

Fig. 1. (A) Muscle strain amplitude *versus* tailbeat frequency. Strain was recorded as the percentage change in resting muscle fibre length (±% l_0) at 0.35, 0.5 and 0.65*BL*, where *BL* is total body length from the rostral tip, over tailbeat frequencies from 1.5 to 2.7 Hz. Measurements from different fish are shown by different symbols: 0.35, 0.5 and 0.65*BL* are shown as open, shaded and filled symbols respectively. There was no correlation between strain and tailbeat frequency. (B) Mean strain amplitude (± S.E.M.) at 0.35, 0.5 and 0.65*BL* (N=3–4 fish at each position). Strain amplitude was significantly different between body positions (P<0.001).

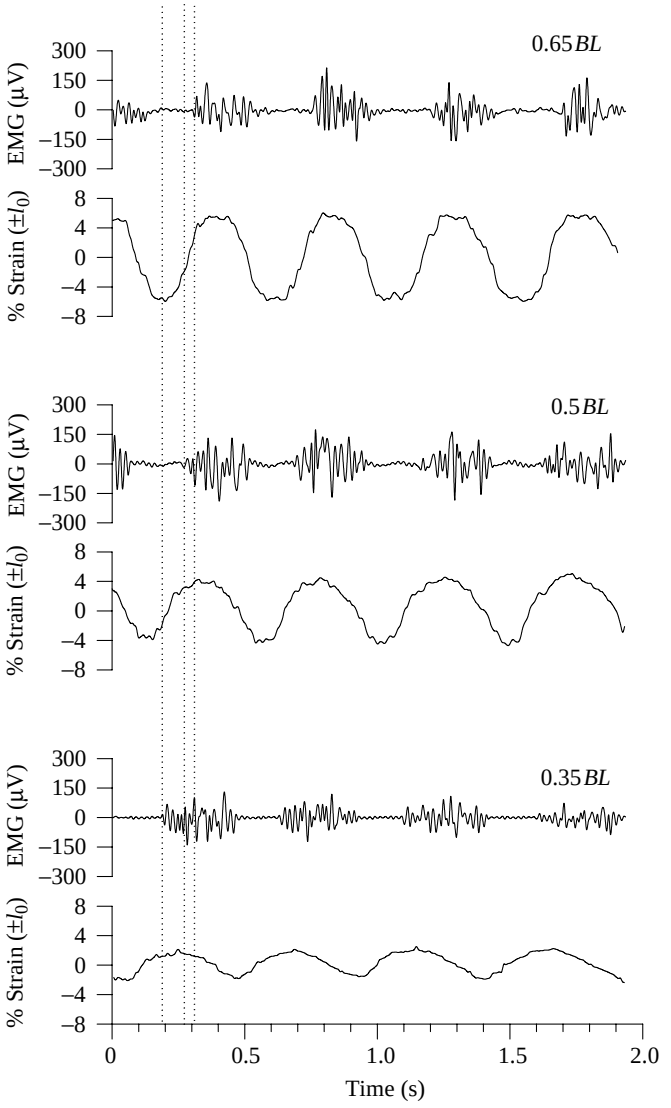

Fig. 2. Three tailbeats of steady swimming at a tailbeat frequency of 2.2 Hz from a 0.38 m total length (*BL*) trout showing simultaneous strain and EMG records from slow muscle at 0.35, 0.5 and 0.65*BL*. The phase relationship between strain and activation changes along the length of the fish so that EMG onset (indicated by vertical dotted lines) is earlier at more caudal positions. EMG offset progresses along the body at a faster rate than onset. l_0, resting muscle fibre length.

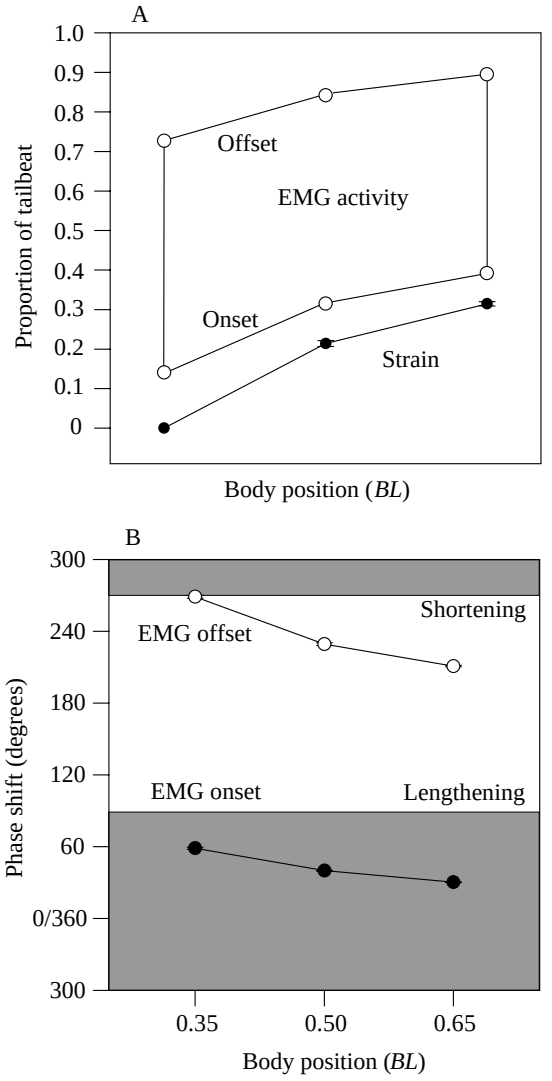

Fig. 3. (A) Speed of the waves of strain (N=3–4; mean ± S.E.M.) and EMG onset and offset (N=3–4) along the fish body. All points are means relative to a time 'zero', when muscle at 0.35*BL* is at l_0 whilst lengthening (i.e. 0 °/360 ° on the strain cycle). Both strain and EMG waves accelerate down the length of the body but the EMG wave travels faster than the strain wave, causing a phase difference between them. (B) The relationship between EMG activity and strain cycle in slow muscle at each of the body positions studied (N=3–4 at each position). The phase (mean ± S.E.M.) of EMG onset (filled circles) and offset (open circles) in relation to the strain cycle are shown assuming that the muscle length change approximates a sine wave. Muscle resting lengths are 0/360 ° and 180 ° on the strain cycle as muscle lengthens and shortens, respectively. *BL*, total length; l_0, resting muscle fibre length.

181±0.6 ° at 0.65*BL* (Fig. 3). Hence, the offset of activation was not simultaneous along the length of the body but progressed from head to tail at a higher velocity than did activation onset.

Mechanical properties of slow muscle

The mechanical properties of slow muscle are summarised in Table 1. Maximum isometric stresses were not significantly different between the three locations. Although twitch rise time t_a slowed from rostral to caudal myotomes (P<0.05), values were not significantly different between mid and caudal myotomes. There was no difference in overall twitch times (t_{90}). Using strains of ±3, 4 and 5 % l_0 at 0.35, 0.5 and 0.65*BL*, respectively, maximum mass-specific power output was not significantly different (P>0.05) between each body position.

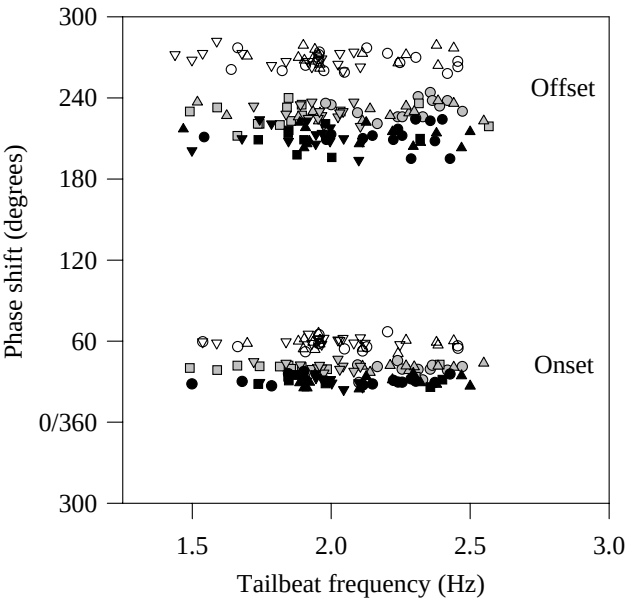

Fig. 4. The relationship between the phase of EMG onset and offset within the strain cycle over a range of tailbeat frequencies. Values from different fish are shown by different symbols. 0.35, 0.5 and 0.65*BL*, where *BL* is total body length, are shown as open, shaded and filled symbols respectively. There was no correlation between tailbeat frequency and phase shift of EMG onset or offset.

Conditions for maximum work and power output

Sinusoidal oscillations were imposed on muscle preparations over a range of frequencies from 0.5 to 6 Hz. As cycle frequency increased, net work decreased (Fig. 5A). At 6 Hz and above, net work was negative for preparations from every body position under all conditions used. Power output increased to a maximum level at 2 Hz and then decreased as cycle frequency increased (Fig. 5B).

At every body position, maximum power output was generated when stimulation began late in the lengthening phase and finished before it was fully shortened (Fig. 6A). When the onset of stimulation occurred during muscle shortening (i.e. at phase shifts between 90 and 270 °) and continued for half the strain cycle, the muscle was active and generated force during lengthening. This caused the negative work component to be high, and net work and power were negative.

To obtain optimum power output *in vitro*, the stimulus duration decreased from 240 ° at 1 Hz to 80 ° at 5 Hz and was the same at each body position (Fig. 5B). At these durations, the phase shift

Table 1. *Summary of mechanical properties of slow muscle fibres from three locations on the body of rainbow trout, 0.35, 0.5 and 0.65*BL *from the rostral tip*

Mechanical property	Muscle location		
	0.35*BL*	0.5*BL*	0.65*BL*
Time to peak force, t_a (ms)	119±6 (6)	142±9 (6)	153±5 (6)
Time from stimulus to 90 % relaxation, t_{90} (ms)	375±18 (4)	384±20 (5)	385±15 (5)
Twitch to tetanus ratio	0.22±0.03 (5)	0.21±0.02 (5)	0.23±0.03 (6)
Maximum isometric stress, P_0 (kN m^{-2})	139±5 (6)	140±5 (6)	132±8 (6)
Maximum power output (W kg^{-1}) at strains of ±3, 4 and 5 % l_0	20±2 (5)	17±3 (5)	17±3 (6)

BL, total body length; l_0, resting muscle fibre length.
Values are means ± S.E.M. with the number of observations given in parentheses.
Power outputs were measured at strains of ±3, 4 and 5 % l_0 at 0.35, 0.5 and 0.65*BL*, respectively.
A one-way ANOVA revealed that t_a was significantly different (P<0.05) between muscle at 0.35*BL* and at the other two locations.

for optimum power output decreased with increasing cycle frequency (Fig. 6B) so that the onset of stimulation occurred earlier in the strain cycle. At 2 Hz, maximum power was generated at phase shifts between 340 and 40 °, corresponding to the mid-lengthening phase of the strain cycle (Fig. 6B).

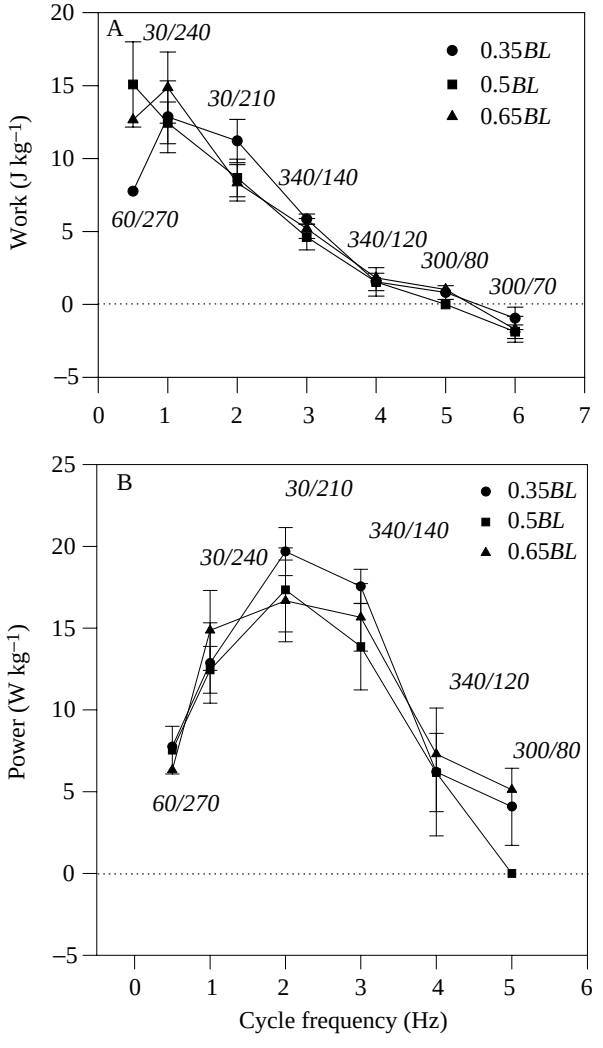

Fig. 5. (A) Net work per cycle and (B) power output plotted against cycle frequency at 9 °C from myotomes at 0.35, 0.5 and 0.65*BL*, where *BL* is total body length from the rostral tip. Values are means ± S.E.M. (*N*=6). Work and power were maximised by changing the phase and duration of stimuli relative to the strain cycle, indicated as *phase*/*duration* (both in degrees) for each frequency. Stimulus onset was earlier in the strain cycle and duration was longer at low frequencies.

In vivo *conditions*

The strains imposed on muscle during this study were estimated from published values because, at the time, the sonomicrometry experiments were in their early stages. However, for mid (0.5*BL*) and rostral (0.65*BL*) positions, these values were the same as the *in vivo* values determined subsequently. Strain amplitude only affects absolute power output (e.g. Altringham and Johnston, 1990; Rome and Swank, 1992; James *et al.* 1995), and the differences between the amplitudes imposed on caudal muscle preparations during this study (±5 % l_0) and those *in vivo* (±6 % l_0) are unlikely to have a significant influence on the results obtained (Altringham and Johnston, 1990).

EMGs are recordings of the muscle action potential (MAP). Once muscle is activated, there is a time lag before force rises that depends on the intrinsic contraction kinetics of the muscle. In an example of a muscle twitch, the lateral muscle of a 30 cm cod *Gadus morhua* (at 14 °C) showed a 5 ms delay before peak EMG activity and a detectable rise in force, and a further 25 ms before force rose to a peak (see Fig. 1 in Wardle, 1985). Although the timing of EMG activity is not synonymous with the timing of muscle stimulation, the time difference by which stimulation precedes EMG activity would be at most 1.5 ° of the strain cycle at the low cycle frequencies imposed on preparations in this study. Therefore, the stimulus timings imposed on muscle in the *in vivo* simulations were taken as approximations of the phase shifts of EMG activity recorded *in vivo*.

At low cycle frequencies, near-maximum power output at 0.5 and 0.65*BL* was achieved at the phase shifts and stimulus

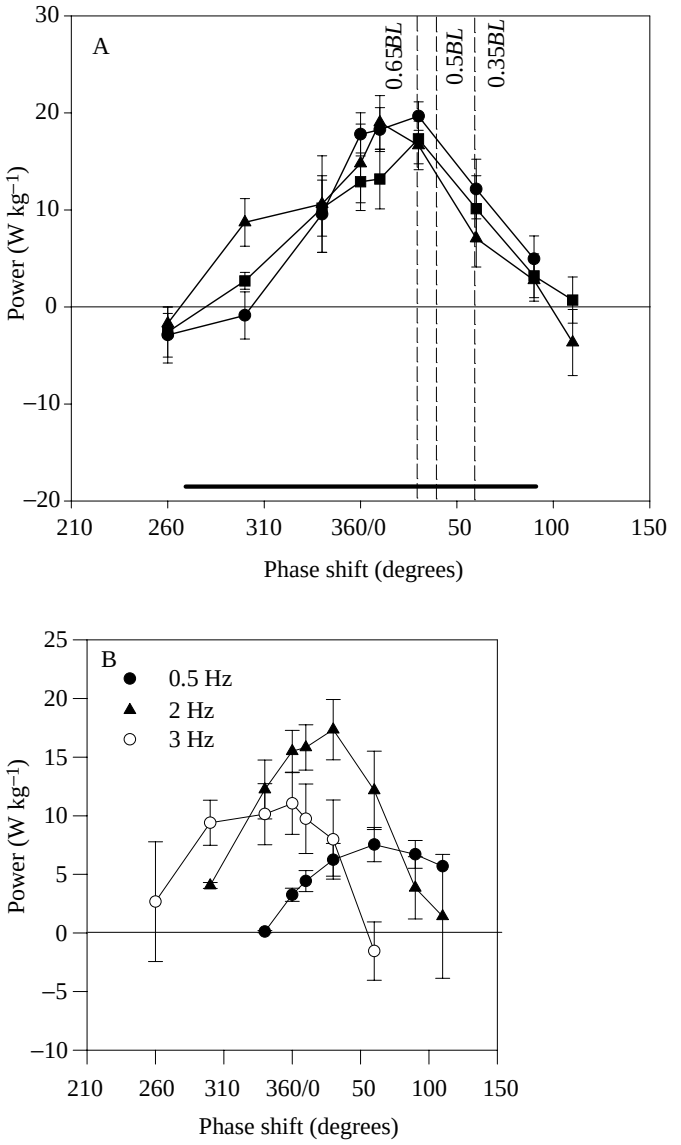

Fig. 6. (A) Mean power output (± S.E.M.) *versus* phase shift at a cycle frequency of 2 Hz (*N*=6). Circles, 0.35*BL*; squares, 0.5*BL*; triangles, 0.65*BL*, where *BL* is total body length of the fish. Stimulus duration was constant at each stimulus phase shift and occupied 180 ° of the strain cycle. The horizontal bar indicates muscle lengthening. Vertical dashed lines show phase shifts for EMG onset measured *in vivo*. (B) Mean power output (± S.E.M.) *versus* stimulus phase shift from preparations at 0.5*BL* (*N*=6). Each curve is at a different cycle frequency (0.5, 2 and 3 Hz). Stimulus duration was constant for each frequency and occupied 210 °, 180 ° and 160 ° of the strain cycle at 0.5, 2 and 3 Hz respectively. The phase shift for optimum power output occurs earlier in the lengthening phase with increased cycle frequency.

durations recorded *in vivo* (Fig. 7). However, under *in vivo* conditions, maximum power output in rostral myotomes was approximately 60 % of the maximum achievable under optimal conditions (Fig. 7). At cycle frequencies above those yielding maximum power (i.e. >2 Hz), stimulus onset must occur earlier than that *in vivo* and stimulus duration must be decreased in order to generate optimal power (Figs 5, 6). However, at these frequencies, optimal power output is less than maximal and differs little from that generated at *in vivo* phase shifts and stimulus durations (Fig. 7).

Fig. 8A shows stress and strain cycles at a cycling frequency of 2 Hz for all three body regions, under strain and stimulation patterns recorded *in vivo*. As a fish swims, the wave of bending travels down the fish in a caudal direction. Therefore, records from 0.5 and 0.65*BL* were offset by 67 ° and 111 °, respectively, relative to the rostral preparation, to simulate the passage of this wave. Force peaked sequentially along the body length. Maximum stress in caudal myotomes was almost twice that of mid and rostral myotomes. Under *in vivo* conditions, force generation occurred primarily during shortening in preparations from all three positions, so muscle performed largely positive work. In rostral myotomes, force rose during lengthening but reached a peak after muscle shortening had started, so that force was generated largely during shortening and muscle performed positive work. In caudal myotomes, muscle activity began earlier in the strain cycle. Although force also rose during lengthening, it reached a peak before muscle reached its maximum length. Therefore, a larger proportion of the force generated was during the lengthening phase, reducing the net positive work performed. The negative work component was typically 45 % of the positive work performed during the cycle. Mid-point myotomes showed an intermediate pattern of force within the strain cycle.

Fig. 8B shows the force and strain records over four cycles for preparations at all three body regions, under conditions approximating those derived from Williams *et al.* (1989). Compared with EMG timings measured in the present study, EMG activity starts much later in the strain cycle at all positions, and EMG duration is significantly shorter in caudal myotomes. Consequently, the pattern of force generation is quite different. At 0.35*BL*, stimulation onset is at 130 ° and continues until muscle is fully shortened (260 °). Force is therefore at its highest as muscle reaches its minimum length and stimulation ceases. However, as muscle relengthens, force is still high as the muscle relaxes and consequently negative work is done. In caudal myotomes, stimulation onset occurs as muscle reaches its maximum length and ends as it shortens through l_0 (i.e. between 90 ° and 180 °). Force rises during shortening and falls before muscle is fully shortened so that most of the force is generated during shortening.

Instantaneous power output

Under the *in vivo* conditions recorded in the present study, the pattern of instantaneous power generation throughout the tailbeat cycle was very similar at each body position (Fig. 9A). Stimulation onset occurred once muscle had lengthened through l_0 so that muscle was active before it reached maximum length. Stretch of active muscle caused negative work to be done, and instantaneous power fell below zero. Stimulation continued as muscle shortened through l_0 and ceased before it was fully shortened. Therefore, as muscle

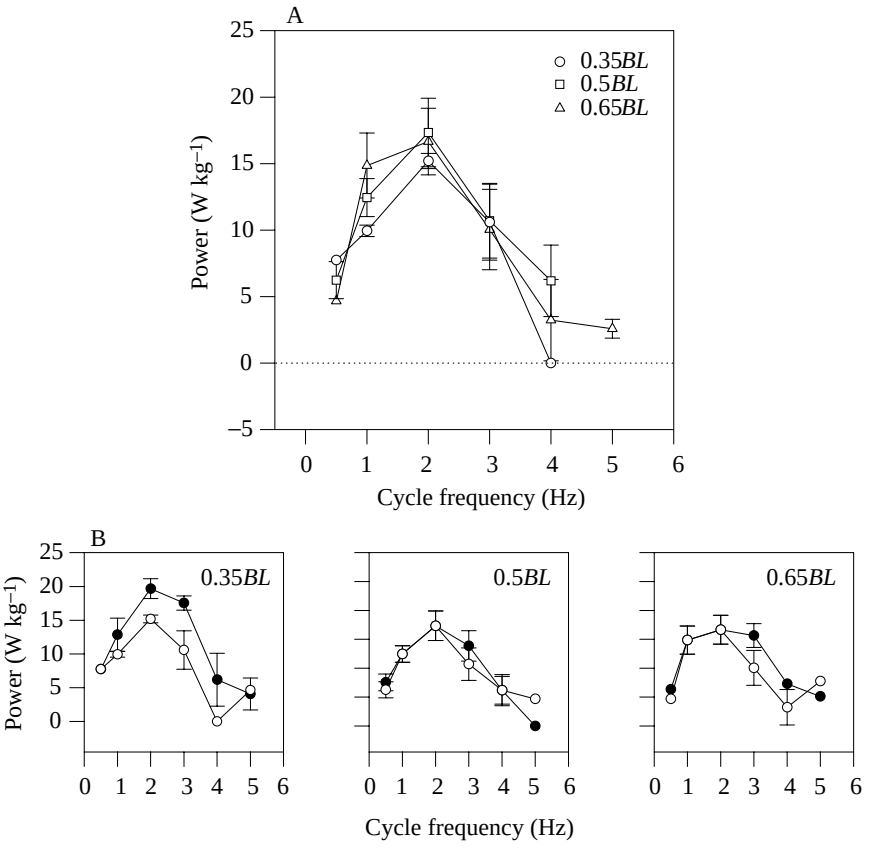

Fig. 7. (A) Power output *versus* cycle frequency at 9 °C from myotomes at 0.35, 0.5 and 0.65*BL* from the rostral tip, where *BL* is total body length. Values are means ± S.E.M. (*N*=6). Stimulus phase shifts and durations were those recorded *in vivo*. The timing and duration of stimulation within the strain cycle were constant for a given body position at all cycle frequencies. From head to tail, stimulus phase shift/stimulus duration was 60 °/210 °, 40 °/190 ° and 30 °/180 °, respectively. (B) Power output *versus* cycle frequency at 9 °C from myotomes at 0.35, 0.5 and 0.65*BL* from the rostral tip. Values are means ± S.E.M. (*N*=6). Power was determined under optimal conditions (filled circles) and *in vivo* conditions (open circles).

shortened, force was high and positive work was performed. Instantaneous power output increased to a peak and then decayed as force declined. Once muscle was fully shortened, activity ceased and instantaneous power fell to zero. Inactive muscle was then relengthened, and the cycles of force, work and power were repeated.

Considering the three positions simultaneously, instantaneous power peaked sequentially from rostral to caudal myotomes (Fig. 9A). Force reached a peak at 0.65*BL* as muscle lengthened, causing instantaneous power output in these myotomes to fall below zero, which coincided with peak instantaneous power at 0.35*BL*. In contrast to the maximum force, peak power was much lower in caudal myotomes and the negative work component was larger. Under these *in vivo* conditions, net positive work per cycle was therefore less in caudal than rostral myotomes.

In contrast, the *in vivo* conditions measured by Williams *et al*. (1989) gave a different pattern of instantaneous power output (Fig. 9B). In all myotomes, the onset of stimulation occurred during muscle shortening so that force rose as muscle shortened and positive work was done. In rostral myotomes, force was highest once muscle had reached minimum length. Consequently, force was generated late in shortening, very little positive work was done and instantaneous power was low. As force remained high once muscle began to relengthen, negative work was done and net work per cycle was negative. In more caudal myotomes, stimulation onset occurred at the start of shortening from maximum length and finished as muscle shortened through l_0. During the shortening phase, force rose and decayed, positive work was done and instantaneous power was high (Fig. 9B). However, considering the three points simultaneously, mid and rostral myotomes perform little useful work and the sequential transfer of peak power along the body is less evident.

Discussion

Kinematics and muscle activity

Our results confirm that slow muscle is used up to a tailbeat frequency of 2.7 Hz, normal for this size of fish (Hudson, 1973). Over tailbeat frequencies between 1.5 and 2.7 Hz, there was no significant increase in strain amplitude, but this may reflect the very limited range of speeds studied.

Muscle strain increased from rostral to caudal positions, as observed in other fish species (e.g. Gray, 1933*a*). Strains were comparable with those measured during steady swimming in a number of carangiform fish (saithe *Pollachius virens*, Hess and Videler, 1984; carp *Cyprinus carpio*, van Leeuwen *et al.* 1990; scup *Stenotomus chrysops*, Rome and Swank, 1992; Rome *et al*. 1993; largemouth bass *Micropterus salmoides*, Jayne and Lauder, 1995).

The bending wave accelerated as it travelled from rostral to caudal positions. However, this is unlikely to influence the relationship between muscle strain and activation timings to the extent that muscle function would alter significantly. Measurements in saithe *Pollachius virens* (L. Hammond, J. D.

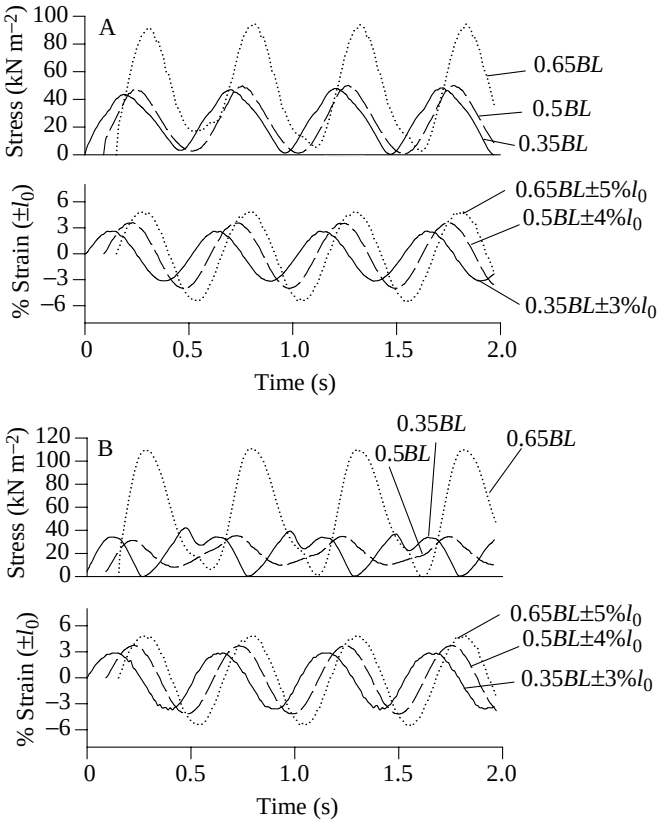

Fig. 8. Muscle strain and stress recordings from four oscillatory cycles at 2 Hz. Recordings are from preparations at three body positions (0.35*BL*, solid line; 0.5*BL*, dashed line; 0.65*BL*, dotted line, where *BL* is total body length). Strain and stimulation variables simulate the conditions predicted for steady-state swimming (A) by this study and (B) from data derived from Williams *et al.* (1989). The strain cycles at 0.5*BL* and 0.65*BL* lag that at 0.35*BL* by 67 ° and 111 °, respectively, as measured *in vivo*. l_0, resting muscle fibre length.

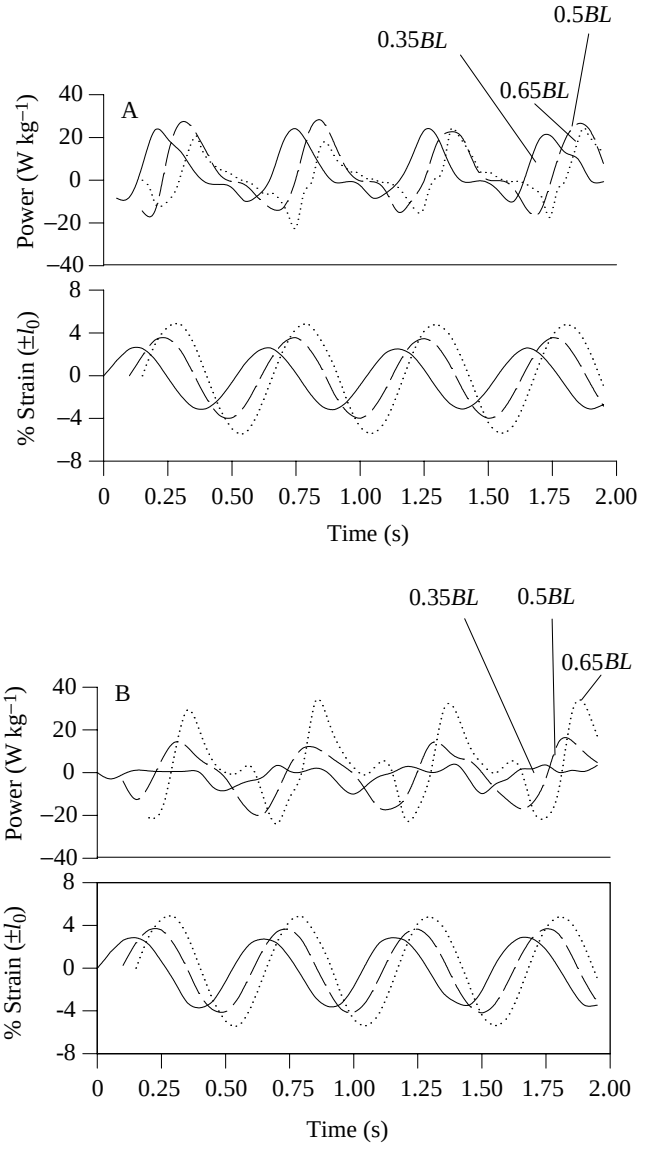

Fig. 9. Instantaneous power output and corresponding strain recordings over three oscillatory cycles at 2 Hz. Recordings are from preparations at three body positions (0.35*BL*, solid line; 0.5*BL*, dashed line; 0.65*BL*, dotted line, where *BL* is total body length). Strain and stimulation parameters were those recorded (A) in this study and (B) from data derived from Williams *et al.* (1989).

Altringham, and C. S. Wardle, in preparation) show a similar bending wave acceleration. Webb *et al.* (1984) reported that the wave of curvature travels at constant speed in rainbow trout, although their technique may not have detected the difference we report here. It may also be the case that the waves of muscle strain and body curvature take different forms. The wave of activation also accelerated along the fish, in constrast to the constant velocity reported for carp *Cyprinus carpio* (van Leeuwen *et al.* 1990). The wave of activation travelled faster than the bending wave, as observed in other species of undulatory swimming fish (eel *Anguilla anguilla*, Grillner and Kashin, 1976; lamprey *Lampetra fluviatilis*, Williams *et al.* 1989; carp *Cyprinus carpio*, van Leeuwen *et al.* 1990; scup *Stenotomus chrysops*, Rome *et al.* 1993; saithe *Pollachius virens*, Altringham *et al.* 1993; saithe and mackerel *Scomber scombrus*, Wardle and Videler, 1993; largemouth bass *Micropterus salmoides*, Jayne and Lauder, 1995).

In vivo *muscle function*

Our results show that at all three locations on the body EMG activity began late in lengthening and finished before muscle was re-extended. The speed of the wave of activity exceeded that of the bending wave, causing a change in the phase shift between them along the body length so that EMG onset occurred earlier in the lengthening phase in more caudal myotomes, at every tailbeat frequency. Moving caudally, EMG activity occupied a smaller proportion of the strain cycle, causing muscle activity to cease before muscle was fully shortened at every position. When muscles were subjected to these *in vivo* activation timings over the functionally important range of swimming frequencies, power output was near optimal at every position.

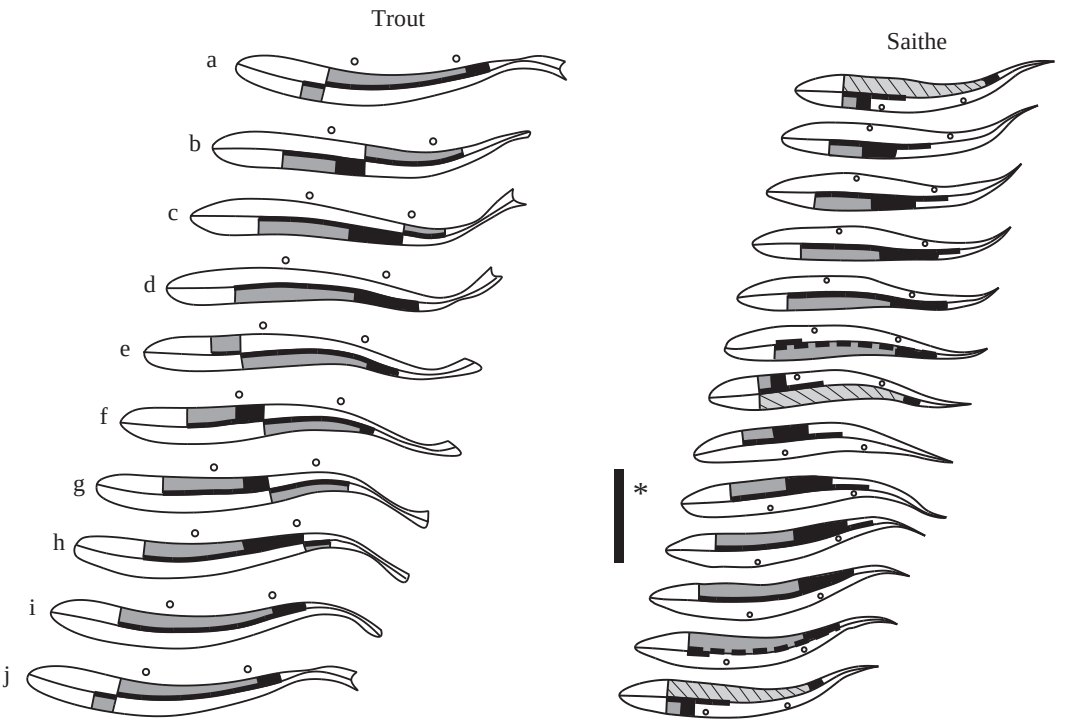

Fig. 10. A schematic representation of the events of a single tailbeat in the rainbow trout *Oncorhynchus mykiss* (2 Hz) and the saithe *Pollachius virens* (18 Hz from Altringham *et al.* 1993), showing progressive fish outlines and midlines in 30 ° increments (where 360 ° represents one tailbeat). EMG activity is shown by the thick black line on either side of the midline. The broken thick black line indicates the moment at which EMG activity stops. Shaded areas indicate that force in that segment is more than 50 % of the maximum force developed in the cycle, during lengthening (black) and shortening (grey). Hatched areas show where muscle force is falling below 50 % of maximum. Circles mark 0.35 and 0.65*BL* from the rostral tip, where *BL* is total body length. The vertical black bar indicates the time of maximum bending moment along the body (Cheng *et al.* 1998). The asterisk indicates the time of peak power at 0.35*BL* and peak force at 0.65*BL*. For further explanation see text.

When preparations were subject to the *in vivo* EMG and strain patterns derived from Williams *et al.* (1989), work done was mainly negative and little, if any, power was generated. EMG activity in all but the most caudal (0.65*BL*) myotomes occurred as the muscle shortened and continued until muscle was fully shortened (i.e. from 90 ° to 270 °). We think it is unlikely that the patterns derived from Williams *et al.* (1989) reflect steady swimming: their fish may have been braking or adjusting its position in the flume.

Thrust generation and body form

Patterns in strain and activity cycles in different species can be related to body form (Wardle *et al.* 1995). In species with tail blades (e.g. carp, saithe, mackerel), the wave of activation is faster than the bending wave, and EMG offset is approximately synchronous along the body length (van Leeuwen *et al.* 1990; Wardle and Videler, 1993). This results in muscle activation occurring over a progressively earlier part of the lengthening phase and for a shorter proportion of the muscle strain cycle from rostral to caudal positions. In contrast, species without tail blades (e.g. eel and lamprey) have a wave of EMG onset that travels only slightly faster than the bending wave and has a progressive EMG offset (Grillner and Kashin, 1976; Williams *et al.* 1989). Therefore, muscle activation occurs over approximately the same portion of the strain cycle at each body position.

The activation timings recorded in rainbow trout during the present study were intermediate between these two patterns and fit well with the trends hypothesised by Wardle *et al.* (1995). As in other species with tail blades, muscle activation occurs earlier in the length change cycle at more posterior regions of the body. Although the duration of activation decreases from rostral to caudal positions, the offset of activation is progressive along the body length. In common with species such as the eel, this results in muscle activity continuing for half the tailbeat cycle at all positions rather than just rostrally, as seen in the saithe. In this way, when muscle is active on one side of the fish, muscle on the opposite side is inactive, and *vice versa*.

Fish with tail blades

Fish with tail blades swim with one or fewer waves of curvature on the body (Webb, 1971; Wardle *et al.* 1995). Thrust is generated as discrete pulses with instantaneous maximum bending moments on alternate sides of the body as the tail or peduncle crosses the fish's track (Lighthill, 1971; Hess and Videler, 1984; Cheng *et al.* 1998). Muscle function changes along the fish length (van Leeuwen *et al.* 1990; Altringham *et al.* 1993; Rome *et al.* 1993): myotomal muscle towards the tail performs negative work for part of the tailbeat cycle. The timing of negative work production in the posterior of the fish coincides with the power-generating phase in rostral myotomes. Consequently, power generated rostrally is transferred to stiffened caudal muscle and passive transmitters, such as septa and backbone, and is passed to the water from the tail blade (Altringham *et al.* 1993; Wardle *et al.* 1995).

Fish without tail blades

In contrast, species without tail blades have 1–1.5 waves of curvature along their body length (Gray, 1933*a*,*b*; Grillner and Kashin, 1976; Williams *et al.* 1989; Hess, 1983). The angle that the body makes with the water causes the fish to deflect water backwards and thus thrust is passed to the water continuously by undulations from head to tail (Gray, 1933*b*). There are no major differences in phase relationship between strain and EMG cycles along the body length (Grillner and Kashin, 1976; Williams *et al.* 1989), suggesting that the mode of muscle function is similar in rostral and caudal myotomes. Power generated by muscle will be passed directly to the water along most of the body length.

Rainbow trout

Fig. 10 shows schematic representations of the events of a single tailbeat for the rainbow trout (this study) and saithe (Altringham *et al.* 1993). During a tailbeat in the saithe, a sequential recruitment of power generators occurs along the body length. Rostrally, active muscle shortens and generates power (grey shading). In caudal myotomes, positive power output is preceded by a period of negative work, during which time muscle is at its maximum stiffness and resists stretch (black shading). At this time, rostral power generation is at a maximum and caudal muscle initially acts to transmit power to the tail blade. A transition zone in which the muscle's role changes from power transmitter to power generator travels caudally during each tailbeat (see also van Leeuwen *et al.* 1990). All muscle contributes to the movement of the tail blade by transferring power through stiffened caudal muscle in addition to through passive elements. Peak power rostrally coincides with peak caudal force as the caudal peduncle crosses the swimming track and generates maximum thrust (Cheng *et al.* 1998). Muscle is then switched off simultaneously along the body length and the same pattern of power generation and transmission occurs along the opposite side of the body. This hypothesised transmission of muscle power down the body to the tail is consistent with widely accepted theories on steady carangiform swimming, which show that thrust is developed largely at the tail blade (Lighthill, 1971).

However, the rainbow trout is a little different. As in the saithe, muscle function changes along the length of the fish. Caudal myotomes go through a phase in which muscle resists stretch and transfers power to the tail blade. However, activation of myotomes in the trout occurs 30 ° later in the strain cycle than in the saithe and continues for approximately half the tailbeat cycle and for almost the same duration at each position. Caudal muscle of the trout is therefore active later in the strain cycle than it is in the saithe. Consequently, force rises later during lengthening and remains high during shortening, causing relatively more positive compared with negative work to be performed in a tailbeat cycle than is performed in saithe muscle at the same position (Fig. 10). This can be seen in the similar pattern of instantaneous power output at each body position (Fig. 9).

A major difference between the saithe and the rainbow trout reflects the inclusion of more than one wave of bending within the body length and results in simultaneous force generation on both sides of the trout for part of the tailbeat cycle (Fig. 10 for the trout, all frames except d and i). When caudally placed muscle on the right side of the fish is pulling the tail blade to the right, rostral muscle on the left is generating power. Power generation on the left will be used primarily to pull the tail blade to the left, but a small component of the rostrally generated power may initially be passed directly to the water by the body wall as hydrodynamic thrust. It would be worthwhile looking for this component in kinematic/hydrodynamic studies.

We would like to thank all those colleagues at Leeds and Aberdeen who assisted us in various ways during these experiments. L.H. was funded by a BBSRC/CASE studentship, with the SOAEFD laboratory as the CASE partner. J.D.A. is grateful to the BBSRC and the Royal Society for support for fish swimming studies

References

ALTRINGHAM, J. D. AND BLOCK, B. A. (1997). Why do tuna maintain elevated slow muscle temperatures? Power output of muscle isolated from endothermic and ectothermic fish. *J. exp. Biol.* **200**, 2617–2627.

ALTRINGHAM, J. D. AND JOHNSTON, I. A. (1990). Modelling muscle power output in a swimming fish. *J. exp. Biol.* **148**, 395–402.

ALTRINGHAM, J. D., WARDLE, C. S. AND SMITH, C. I. (1993). Myotomal muscle function at different locations in the body of a swimming fish. *J. exp. Biol.* **182**, 191–206.

CARLING, J. C., BOWTELL, G. AND WILLIAMS, T. L. (1994). Anguilliform body dynamics: a continuum model for the interaction between muscle activation and body curvature. In *Mechanics and Physiology of Animal Swimming* (ed. L. Maddock, Q. Bone and J. M. V. Rayner), pp. 119–132. Cambridge: Cambridge University Press.

CHENG, J.-Y., PEDLEY, T. J. AND ALTRINGHAM, J. D. (1998). A continuous dynamic model for swimming fish. *Phil. Trans R. Soc. B* (in press).

GOLDMAN, D. E. AND RICHARDS, J. R. (1954). Measurement of high frequency sound velocity in mammalian soft tissues. *J. acoust. Soc. Am.* **26**, 981–983.

GRAY, J. (1933*a*). Studies in animal locomotion. I. The movement of the fish with special reference to the eel. *J. exp. Biol.* **10**, 88–104.

GRAY, J. (1933*b*). Studies in animal locomotion. II. The relationship between waves of muscular contraction and the propulsive mechanism of the eel. *J. exp. Biol.* **10**, 386–390.

GRIFFITHS, R. I. (1987). Ultrasound transit time gives direct measurement of muscle fibre length *in vivo*. *J. Neurosci. Meth.* **21**, 159–165.

GRILLNER, S. AND KASHIN, S. (1976). On the generation and performance of swimming in fish. In *Neural Control of Locomotion* (ed. R. M. Herman, S. Grillner, P. S. G. Stein and D. G. Stuart), pp. 181–201. New York: Plenum.

HATTA, I., SUGI, H. AND TAMURA, Y. (1988). Stiffness changes in frog skeletal muscle during contraction recorded using ultrasonic waves. *J. Physiol., Lond.* **403**, 193–209.

HESS, F. (1983). Bending moments and muscle power in swimming fish. *Proceedings of the Eighth Australian Fluid Mechanics Conference* **2**, 12A1–12A3. Newcastle, NSW.

HESS, F. AND VIDELER, J. J. (1984). Fast continuous swimming of saithe: a dynamic analysis of bending moments and muscle power. *J. exp. Biol.* **109**, 229–251.

HUDSON, R. C. L. (1973). On the function of the white muscles in teleosts at intermediate swimming speeds. *J. exp. Biol.* **58**, 509–522.

JAMES, R. S., ALTRINGHAM, J. D. AND GOLDSPINK, D. F. (1995). The mechanical properties of fast and slow skeletal muscles of the mouse in relation to their locomotory function. *J. exp. Biol.* **198**, 491–502.

JAYNE, B. C. AND LAUDER, G. V. (1995). Red muscle motor patterns during steady swimming in largemouth bass: effects of speed and correlations with axial kinematics. *J. exp. Biol.* **198**, 1575–1587.

JOSEPHSON, R. K. (1985). Mechanical power output from striated muscle during cyclic contraction. *J. exp. Biol.* **114**, 493–512.

JOSEPHSON, R. K. (1993). Contraction dynamics and power output of skeletal muscle. *A. Rev. Physiol.* **55**, 527–546.

LIGHTHILL, M. J. (1971). Large amplitude elongated body theory of fish locomotion. *Proc. R. Soc. B* **179**, 125–138.

MOI, C. R. AND BREDDELS, P. A. (1982). Ultrasound velocity in muscle. *J. acoust. Soc. Am.* **71**, 455–461.

ROME, L. C. AND SWANK, D. (1992). The influence of temperature on power output of scup red muscle during cyclical length changes. *J. exp. Biol.* **171**, 261–281.

ROME, L. C., SWANK, D. AND CORDA, D. (1993). How fish power swimming. *Science* **261**, 340–343.

VAN LEEUWEN, J. L., LANKHEET, M. J. M., AKSTER, H. A. AND OSSE, J. W. M. (1990). Function of red axial muscles of carp (*Cyprinus carpio*): recruitment and normalized power output during swimming in different modes. *J. Zool., Lond.* **220**, 123–145.

WARDLE, C. S. (1985). Swimming activity in marine fish. In *Physiological Adaptations of Marine Animals* (ed. M. S. Laverack), pp. 521–540. Cambridge: The Company of Biologists.

WARDLE, C. S. AND VIDELER, J. J. (1993). The timing of the EMG in lateral myotomes of mackerel and saithe at different swimming speeds. *J. Fish Biol.* **42**, 347–359.

WARDLE, C. S., VIDELER, J. J. AND ALTRINGHAM, J. D. (1995). Tuning into fish swimming waves: body form, swimming mode and muscle function. *J. exp. Biol.* **198**, 1629–1636.

WEBB, P. W. (1971). The swimming energetics of trout. I. Thrust and power output at cruising speeds. *J. exp. Biol.* **55**, 489–520.

WEBB, P. W. (1988). Steady swimming kinematics of tiger musky, an esociform accelerator and rainbow trout, a generalist cruiser. *J. exp. Biol.* **138**, 51–69.

WEBB, P. W., KOSTECKI, P. T. AND STEVENS, E. D. (1984). The effect of size and swimming speed on locomotion kinematics of rainbow trout. *J. exp. Biol.* **109**, 77–95.

WILLIAMS, T. L., GRILLNER, S., SMOLJANINOV, V. V., WALLEN, P., KASHIN, S. AND ROSSIGNOL, S. (1989). Locomotion in lamprey and trout: the relative timing of activation and movement. *J. exp. Biol.* **143**, 559–566.